Novel Effect of Zinc Nitrate/Vanadyl Oxalate for Selective Catalytic Oxidation of α-Hydroxy Esters to α-Keto Esters with Molecular Oxygen: An In Situ ATR-IR Study

Yongwei Ju [1], Zhongtian Du [2,*], Chuhong Xiao [2], Xingfei Li [2] and Shuang Li [1,*]

[1]   School of Chemical Engineering, Northwest University, Xi'an 710069, China; 201620730@stumail.nwu.edu.cn
[2]   School of Petroleum and Chemical Engineering, Dalian University of Technology, Panjin 124221, China;
     xiaochuhong@mail.dlut.edu.cn (C.X.); lixingfei620@mail.dlut.edu.cn (X.L.)
*   Correspondence: duzhongtian@dlut.edu.cn (Z.D.); shuangli722@126.com (S.L.); Tel.: +86-029-88303733 (S.L.)

check for
updates

Abstract: Selective oxidation of α-hydroxy esters is one of the most important methods to prepare high value-added α-keto esters. An efficient catalytic system consisting of $Zn(NO_3)_2/VOC_2O_4$ is reported for catalytic oxidation of α-hydroxy esters with molecular oxygen. Up to 99% conversion of methyl DL-mandelate or methyl lactate could be facilely obtained with high selectivity for its corresponding α-keto ester under mild reaction conditions. $Zn(NO_3)_2$ exhibited higher catalytic activity in combination with VOC_2O_4 compared with $Fe(NO_3)_3$ and different nitric oxidative gases were detected by situ attenuated total reflection infrared (ATR-IR) spectroscopy. UV-vis and ATR-IR results indicated that coordination complex formed in $Zn(NO_3)_2$ in CH_3CN solution was quite different from $Fe(NO_3)_3$; it is proposed that the charge-transfer from Zn^{2+} to coordinated nitrate groups might account for the generation of different nitric oxidative gases. The XPS result indicate that nitric oxidative gas derived from the interaction of $Zn(NO_3)_2$ with VOC_2O_4 could be in favor of oxidizing VOC_2O_4 to generate active vanadium (V) species. It might account for different catalytic activity of $Zn(NO_3)_2$ or $Fe(NO_3)_3$ combined with VOC_2O_4. This work contributes to further development of efficient aerobic oxidation under mild reaction conditions.

Keywords: ATR-IR; α-hydroxy esters; α-keto esters; oxidation; zinc nitrate

1. Introduction

α-keto esters, which have two-functional groups, are valuable precursors in a variety of organic transformations [1–3]. For example, phenylglyoxylate and its derivatives are used as key intermediates for synthesis of herbicide metamitron [2], and pyruvate and its derivatives can be employed for the preparation of pharmaceutical pindolol and pesticides thiabendazole [3]. In the past several decades, several methods for synthesis of α-keto esters have been reported, such as esterification of α-keto acids or α-carbonyl aldehydes, oxidative cleavage of β-diketones, oxidative esterification of aryl-ketones and so on [4–6]. Considering the excellent atom efficiency, there is a growing interest to develop efficient catalytic oxidation of α-hydroxy esters into their corresponding α-keto esters [7,8].

Oxidation of α-hydroxy esters into α-keto esters is essentially selective oxidation of a secondary alcohol adjacent to a carboxylic ester group. Due to the inherent steric hindrance and electronic effect, complete conversion of α-hydroxy esters is usually difficult, while oxidative C-C bond cleavage could easily occur between two adjacent carbonyl carbon atoms under harsh oxidative reaction conditions [7,8]. Recently, several efficient aerobic catalytic systems have been developed under mild liquid reaction conditions [9–13], such as Pd-, Au-, and Ru-based catalysts, AZADO-$NaNO_2$ and

TEMPO-NaNO$_2$. We are encouraged by all these methods, although some drawbacks still exist, such as side reactions, and use of expensive organic or metal catalysts. Therefore, it is still rather challenging for efficient catalytic oxidation of α-hydroxy esters into α-keto esters with molecular oxygen under mild reaction conditions.

As a base transitional metal, vanadium catalysts have been uncovered for aerobic oxidation of alcohols to carbonyl compounds recently [14,15]. Kirihara et al. achieved excellent yields of α-keto esters using fuming and corrosive VOCl$_3$ [16]. Hanson et al. described the key role of pyridine during the alcohol oxidation by dipicolinate vanadium (V) [17,18]. Xu et al. also reported efficient catalytic oxidation of 5-hydroxymethylfurfural to furan-2,5-dicarbaldehyde, and C-C bond cleavage could be tuned using different vanadium-based catalysts [19,20]. These reports have provided us with important information concerning the selective oxidation of α-hydroxy esters using vanadium-based catalysts under mild reaction conditions. We used a highly efficient catalytic system consisting of Zn(NO$_3$)$_2$/VOC$_2$O$_4$ for selective oxidation of α-hydroxy esters into α-keto esters with molecular oxygen under mild reaction conditions, and employed infrared spectroscopy to investigate the unique catalytic activity of Zn(NO$_3$)$_2$ compared with other metal nitrates such as Fe(NO$_3$)$_3$.
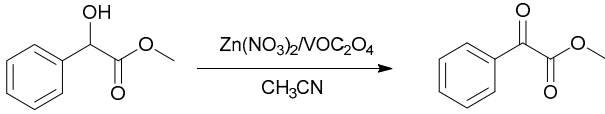
2. Results and Discussion

Initially, oxidation of methyl DL-mandelate with molecular oxygen was selected as a model reaction, and performed in acetonitrile under mild reaction conditions (80 °C, 0.2 MPa O$_2$). Table 1 shows the results on catalytic oxidation of methyl DL-mandelate with different catalysts. Only 5–6% conversion of methyl DL-mandelate was obtained using Zn(NO$_3$)$_2$ or VOC$_2$O$_4$ (Table 1, Entries 1–2). In contrast, 99% methyl phenylglyoxylate selectivity with 99% methyl DL-mandelate conversion was obtained within 1.5 h when both Zn(NO$_3$)$_2$ and VOC$_2$O$_4$ (molar ration = 1) were employed (Table 1, Entry 3). Moreover, no C-C bond cleavage of methyl phenylglyoxylate was observed even by prolonging the reaction time from 1.5 h to 6 h, which suggests that methyl phenylglyoxylate could remain stable under such oxidative environment (Table 1, Entry 4). Furthermore, nearly quantitative yield of methyl phenylglyoxylate could be facilely obtained at room temperature (25 °C) under normal pressure of molecular oxygen (Table 1, Entry 5). Compared with VOCl$_3$ and other vanadium organic complexes [17,18,21–23], Zn(NO$_3$)$_2$/VOC$_2$O$_4$ is inexpensive and halogen free. All these results indicate that the catalytic system of Zn(NO$_3$)$_2$/VOC$_2$O$_4$ was efficient for catalytic oxidation of methyl DL-mandelate into methyl phenylglyoxylate with dioxygen under mild reaction conditions.

Further, we also compared different nitrates for catalytic oxidation of methyl DL-mandelate under the same reaction conditions (Table 1, Entries 6–10). When Co(NO$_3$)$_2$, Ce(NO$_3$)$_3$, Fe(NO$_3$)$_3$, Ni(NO$_3$)$_2$ and NaNO$_3$ were employed instead of Zn(NO$_3$)$_2$, only 8–33% conversion of methyl DL-mandelate was observed. Zn(NO$_3$)$_2$ showed the best performance among those metal nitrates tested in this work. As a typical transition metal nitrate with multi-valences, Fe(NO$_3$)$_3$ was often used as a key component for selective oxidation of alcohols in previous reports [24,25]. Unexpectedly, Fe(NO$_3$)$_3$ displayed much lower catalytic activity than Zn(NO$_3$)$_2$, and only 16% methyl DL-mandelate conversion was obtained using Fe(NO$_3$)$_3$/VOC$_2$O$_4$ as the catalyst under the same reaction conditions. Thus, the nitrates could affect the catalytic activity significantly in this work. This issue is discussed in the following section.

Besides methyl DL-mandelate, lactate esters and benzoin were also oxidized (Table 2). Methyl lactate and ethyl lactate are typical aliphatic α-hydroxy esters, which are more difficult to be oxidized than methyl DL-mandelate. When they were oxidized, 21% and 59% conversion was obtained, respectively, with 99% pyruvate esters selectivity within 1.5 h. To our delight, 99% methyl lactate and ethyl lactate conversion with high selectivity of pyruvate esters was achieved after prolonging the reaction time to 4 h. Furthermore, good yields of pyruvate esters could also be attained at normal pressure of molecular oxygen at room temperature (Table 2, Entries 1–2). Moreover, the selectivity of byproducts (mainly acetic acid) derived from C-C bond cleavage was no more than 3%. As described above, it seemed difficult to obtain high yields of pyruvate directly from lactate via oxidation because of the side formation of CO$_2$ through C−C bond fission [7,8]. For example, only 70% selectivity

towards ethyl pyruvate was obtained when TiO_2 was used for catalytic oxidation of ethyl lactate into ethyl pyruvate under mild reaction conditions [26]. Our results are competitive when compared with that using $VOCl_3$ as a catalyst [27]. More than 95% benzil selectivity with 99% benzoin conversion could be achieved within 4 h. Oxidation of benzoin into benzil could also proceed smoothly under normal pressure of molecular oxygen at room temperature (Table 2, Entry 3). Only 5% benzoic acid/benzaldehyde byproducts were detected. Therefore, $Zn(NO_3)_2/VOC_2O_4$ is effective for catalytic oxidation of α-hydroxy compounds even under normal pressure and room temperature.
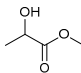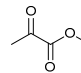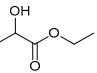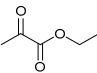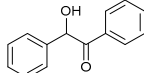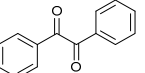
Table 1. Catalytic oxidation of methyl DL-mandelate with different catalyst [a].

Entry	Metal Nitrate	t (h)	Conversion (%)	Selectivity [b] (%)
1	-	1.5	6	>99
2 [c]	$Zn(NO_3)_2$	1.5	5	>99
3	$Zn(NO_3)_2$	1.5	>99	>99
4	$Zn(NO_3)_2$	6	>99	>99
5 [d]	$Zn(NO_3)_2$	48	>99	>99
6	$NaNO_3$	1.5	33	95
7	$Ni(NO_3)_2$	1.5	25	>99
8	$Fe(NO_3)_3$	1.5	16	95
9	$Ce(NO_3)_3$	1.5	11	>99
10	$Co(NO_3)_2$	1.5	8	>99

[a] Reaction conditions: 5 mmol methyl DL-mandelate, 0.25 mmol metal nitrate, 0.25 mmol VOC_2O_4, 5 mL CH_3CN, 80 °C, 0.2 MPa O_2, 1.5 h. [b] Selectivity toward for methyl phenylglyoxylate. [c] No VOC_2O_4 was added. [d] Room temperature, normal pressure using O_2 balloon.

Table 2. Catalytic oxidation of lactate esters and benzoin with $Zn(NO_3)_2/VOC_2O_4$ [a].

Entry	Substrate	Product	t (h)	Conversion (%)	Selectivity (%)
1			1.5	59	99
			4	>99	97
			72 [b]	>99	97
2			1.5	21	99
			4	>99	98
			72 [b]	>99	98
3			1.5	81	96
			4	>99	95
			48 [b]	>99	95

[a] Reaction conditions: 5 mmol substrate, 0.25 mmol $Zn(NO_3)_2$, 0.25 mmol VOC_2O_4, 5 mL CH_3CN, 80 °C, 0.2 MPa O_2. [b] Room temperature, normal pressure using O_2 balloon.

Operando attenuated total reflection infrared (ATR-IR) spectroscopy has been demonstrated as a powerful method to monitor real-time chemical reactions [28].To explore the oxidation process catalyzed by $Zn(NO_3)_2/VOC_2O_4$, oxidation of methyl DL-mandelate was monitored by online ATR-IR (Figure 1). The bands at 1694 and 1742 cm^{-1} were assigned to C=O stretching vibrations of carbonyl (methyl phenylglyoxylate) and esters functional group, respectively. The band at 1096 cm^{-1} was assigned to C-O stretching vibration of methyl DL-mandelate [29]. The signal at 1694 cm^{-1} rose gradually in the beginning, while the peak height at 1096 cm^{-1} (C-O stretching vibration of methyl DL-mandelate) diminished. Methyl DL-mandelate was converted to methyl phenylglyoxylate, and no

other significant intermediates were detected by ATR-IR during the oxidation reaction. Moreover, the peaks at 1742 and 1694 cm^{-1} remained stable as the reaction time prolonged, and no other significant signals appeared, indicating that few byproducts were generated under such oxidative conditions. These observations were in accordance with GC analysis (Table 1).
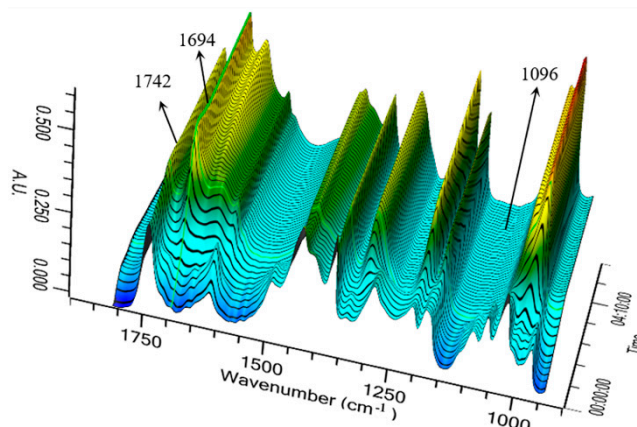

Figure 1. The real-time profile of methyl DL-mandelate oxidation monitored by online ATR-IR. Reaction conditions: 10 mmol methyl DL-mandelate, 1 mmol Zn(NO$_3$)$_2$, 1 mmol VOC$_2$O$_4$, 10 mL CH$_3$CN, 80 °C, O$_2$ balloon.

To explore the different catalytic activities of nitrates, we selected Zn(NO$_3$)$_2$ and Fe(NO$_3$)$_3$ to study the interaction of catalyst components using FT-IR. The reaction of Zn(NO$_3$)$_2$ or Fe(NO$_3$)$_3$ with VOC$_2$O$_4$ was carried out in acetonitrile without methyl DL-mandelate (80 °C, 0.2 MPa O$_2$, 1.5 h). After the pre-treatment, a red brown powder was obtained after removing acetonitrile. The FT-IR spectra are presented in Figure 2. For the FT-IR spectrum of VOC$_2$O$_4$ (Figure 2, Line a), the band at 977 cm^{-1} was attributed to be characteristic of V=O stretching vibration and the 826 cm^{-1} band was due to O-C=C bending and M-O stretching vibration [30]. The shoulder bands at 1390 and 1356 cm^{-1} were assigned to N-O stretching vibrations of Zn(NO$_3$)$_2$ (Figure 2, Line b), while the sharp band at 1386 cm^{-1} was attributed to N-O stretching vibration of Fe(NO$_3$)$_3$ (Figure 2, Line c) [31]. It should be noted that the FT-IR spectrum of reaction mixture derived from Zn(NO$_3$)$_2$/VOC$_2$O$_4$ (Figure 2, Line d) was quite different from those of VOC$_2$O$_4$ or Zn(NO$_3$)$_2$ (Figure 2, Lines a and b). Two new bands at 1326 and 816 cm^{-1} (Figure 2, Line d) appeared while no similar new absorption bands were generated when VOC$_2$O$_4$ was reacted with Fe(NO$_3$)$_3$ under the same reaction conditions (Figure 2, Line e). These results suggest that the reaction mixtures derived from Zn(NO$_3$)$_2$ and Fe(NO$_3$)$_3$/VOC$_2$O$_4$ were quite different, especially the form of nitric species. These phenomena may be related to the generation of different NO$_x$ gases, which might account for catalytic activity difference by using Zn(NO$_3$)$_2$ or Fe(NO$_3$)$_3$ with VOC$_2$O$_4$, respectively.

The observation above was further confirmed by investigating the interaction of Zn(NO$_3$)$_2$ or Fe(NO$_3$)$_3$ with VOC$_2$O$_4$ using online ATR-IR (Figure 3). Firstly, in the absence of substrate, VOC$_2$O$_4$ was stirred at 80 °C in acetonitrile under an oxygen atmosphere, and no apparent variation of spectrum was observed. This observation suggests that VOC$_2$O$_4$ alone remained stable under oxidative reaction conditions. When Zn(NO$_3$)$_2$ was introduced, new bands at 1326 and 816 cm^{-1} were generated simultaneously (Figure 3, top). On the contrary, when Fe(NO$_3$)$_3$ was added under the same reaction conditions, the ATR-IR spectrum (Figure 3, bottom) was distinct from that derived from Zn(NO$_3$)$_2$/VOC$_2$O$_4$. The bands at 1326 and 816 cm^{-1} were not observed (Figure 3, bottom). The online ATR-IR results were in good agreement with FT-IR results (Figure 2). These results demonstrated that different nitric species occurred in liquid phase by adding Zn(NO$_3$)$_2$ or Fe(NO$_3$)$_3$ under such oxidative conditions. This difference might be associated with the generation of NO$_x$ gases. It might account for lower catalytic activity for Fe(NO$_3$)$_3$ than that of Zn(NO$_3$)$_2$.

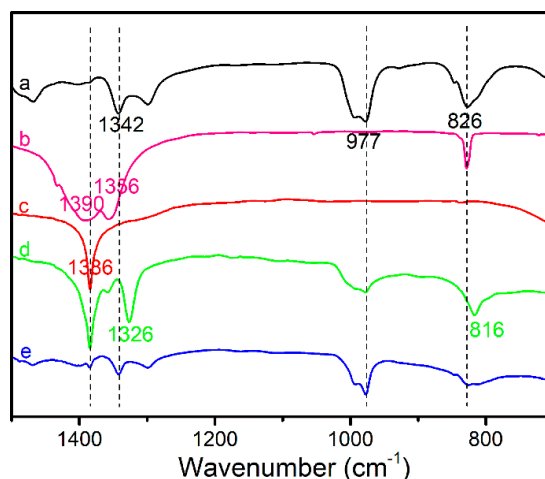**Figure 2.** FT-IR investigation on the interaction of nitrates and VOC_2O_4: (a) VOC_2O_4; (b) $Zn(NO_3)_2$; (c) $Fe(NO_3)_3$; (d) $Zn(NO_3)_2 + VOC_2O_4$, $Zn(NO_3)_2$:VOC_2O_4 = 1:1 (molar ratio), 0.2 MPa O_2, 5 mL CH_3CN, 80 °C, 1.5 h; and (e) $Fe(NO_3)_3 + VOC_2O_4$, $Fe(NO_3)_3$:VOC_2O_4 = 1:1 (molar ratio), 0.2 MPa O_2, 5 mL CH_3CN, 80 °C, 1.5 h.

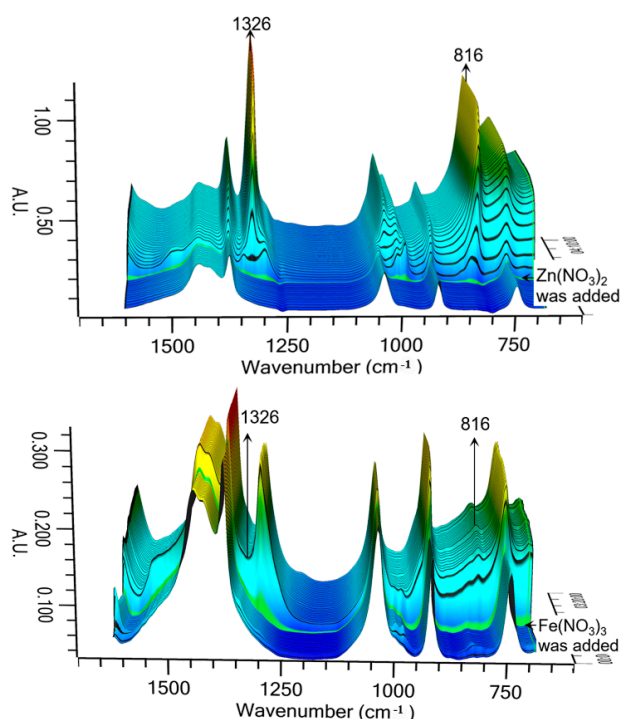**Figure 3.** In situ ATR-IR investigation on interaction of nitrates and VOC_2O_4, nitrates:VOC_2O_4 = 1:1 (molar ratio): Interaction of $Zn(NO_3)_2$ and VOC_2O_4 (**top**); and interaction of $Fe(NO_3)_3$ and VOC_2O_4 (**bottom**).

To verify the hypothesis mentioned above, we employed ATR-IR spectroscopy to detect composition of the gas phase, which was generated from the reaction of $Zn(NO_3)_2$/VOC_2O_4 or $Fe(NO_3)_3$/VOC_2O_4 (Figure 4). Firstly, $Zn(NO_3)_2$/VOC_2O_4 was stirred without the substrate under an oxygen atmosphere at 80 °C. In these experiments, the React IR™ 15-diamond probe was immersed in gas phase rather than liquid phase. The ATR-IR spectrum of gas phase demonstrated that new species which IR bands at 1671, 1305 and 936 cm^{-1} generated were attributable to HNO_3 vapor (Figure 4, Line a) [32]. This observation suggests that HNO_3 vapor probably was involved as one of key components during the oxidation using $Zn(NO_3)_2$/VOC_2O_4. In contrast, when the gas derived

from $Fe(NO_3)_3/VOC_2O_4$ was monitored under the same conditions, IR bands at 1756, 1383, 1211 and 1003 cm^{-1} were detected. These bands were related to N_2O_3 and N_2O_4 mixture gas (Figure 4, Line b) [33,34], which were quite different from those derived from $Zn(NO_3)_2/VOC_2O_4$ (Figure 4, Line a). All these results above indicate that different NO_x gases were involved during catalytic oxidation using $Zn(NO_3)_2/VOC_2O_4$ or $Fe(NO_3)_3/VOC_2O_4$. The obvious difference in NO_x gases generated by using $Zn(NO_3)_2/VOC_2O_4$ or $Fe(NO_3)_3/VOC_2O_4$ was further investigated.
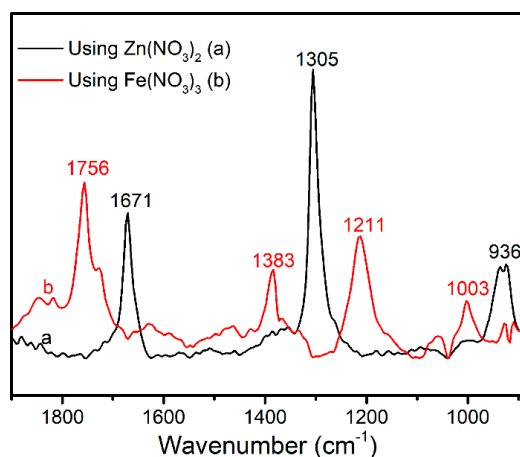

Figure 4. NO_x gas detected by in situ ATR-IR. Reaction conditions: 1 mmol $Zn(NO_3)_2$ or $Fe(NO_3)_3$, 1 mmol VOC_2O_4, 10 mL CH_3CN, 80 °C, O_2 balloon.

UV-vis spectroscopy was employed to detect coordination state of $Zn(NO_3)_2/Fe(NO_3)_3$ in CH_3CN. An intense and broad peak at 293 nm was observed in $Zn(NO_3)_2$ in CH_3CN solution, which was assigned to the n–π* transition, while no obvious peak was found on $Fe(NO_3)_3$ in CH_3CN solution (Figure S2). It is proposed that the observed variation in the UV-vis spectrum should be interpreted as a coordination interaction taking place between $Zn(NO_3)_2$ and CH_3CN solvent [35]. ATR-IR spectra in the C-N region of $Zn(NO_3)_2/Fe(NO_3)_3$ in CH_3CN solution are shown in Figure S3. The bands at 2253 and 2292 cm^{-1} were assigned to C-N stretching vibrations of CH_3CN, a new band at 2314 cm^{-1} appeared as $Zn(NO_3)_2$ was added to CH_3CN, while no new band at 2314 cm^{-1} appeared as $Fe(NO_3)_3$ was added to CH_3CN. This difference could be attributed to the unique complete filled 3d electronic orbitals of Zn^{2+} ($3d^{10}$), which is quite different from Fe^{3+} ($3d^5$) causing vibrations of the coordinated CH_3CN. Previous studies also report a similar $[Zn(CH_3CN)_2](NO_3)_2$ coordination complex forming in $Zn(NO_3)_2$ in CH_3CN solvent [36]. It can be inferred that charge-transfer from Zn^{2+} to coordinated nitrate groups might account for the generation of different NO_x gases using $Zn(NO_3)_2$ and $Fe(NO_3)_3$, respectively [37].

The catalytic system consisting of nitrates and vanadium compounds has been reported, and the cascade electron transfer among nitric, vanadium species and oxygen was proposed [19,20]. vanadium (IV) species could be easily oxidized to vanadium (V) species by nitric oxidative gas rather than oxygen and after that the active vanadium (V) species oxidized alcohol group to ketone. We also believe that similar redox cycles existed in this work. To verify whether this nitric oxidative gas derived from the interaction of $Zn(NO_3)_2$ with VOC_2O_4 could promote the oxidation of VOC_2O_4 to generate active vanadium (V) species. XPS measurements were employed to detect the active vanadium (V) species after the interaction of $Zn(NO_3)_2$ or $Fe(NO_3)_3$ with VOC_2O_4. Firstly, the reaction of $Zn(NO_3)_2$ or $Fe(NO_3)_3$ with VOC_2O_4 was carried out in acetonitrile (80 °C, 0.2 MPa O_2, 1.5 h). The reaction mixture was then obtained after removing acetonitrile. V 2p XPS spectra of the reaction mixture was shown in Figure 5. The peak of vanadium (IV) locates at 516.8 eV and that of vanadium (V) at 517.9 eV, which are in good accordance with previous report (516.5 eV for vanadium (IV) and 517.6 eV for vanadium (V)) [38]. It can be seen that vanadium (V) species appeared after the interaction of $Zn(NO_3)_2$ with VOC_2O_4 (Figure 5, Line a), while no vanadium (V) species existed in the reaction mixture of $Fe(NO_3)_3/VOC_2O_4$ under the

same reaction conditions (Figure 5, Line b). V 2p XPS spectra of the reaction mixture provided strong evidence for the generation of vanadium (V) species in the $Zn(NO_3)_2$/VOC_2O_4 catalytic system. It is known that oxidizing ability of nitric oxidative gas was quite different [39]. Combining ATR-IR with XPS characterization results suggests that HNO_3 gas derived from the interaction of $Zn(NO_3)_2$ with VOC_2O_4 could be in favor of oxidizing vanadium (IV) species to active vanadium (V) species, thus explaining why $Zn(NO_3)_2$ combined with VOC_2O_4 exhibited unique catalytic activity, compared with other tested metal nitrates such as $Fe(NO_3)_3$ under the same reaction conditions.
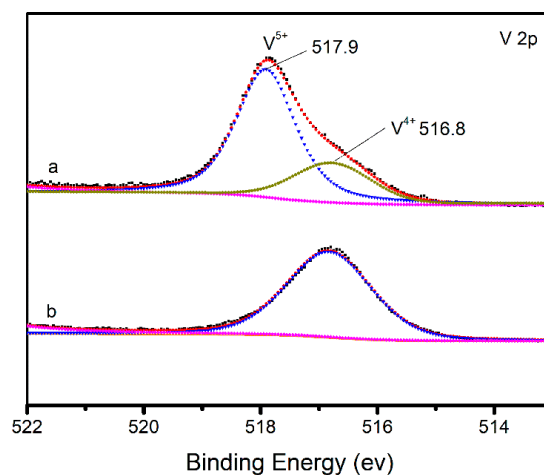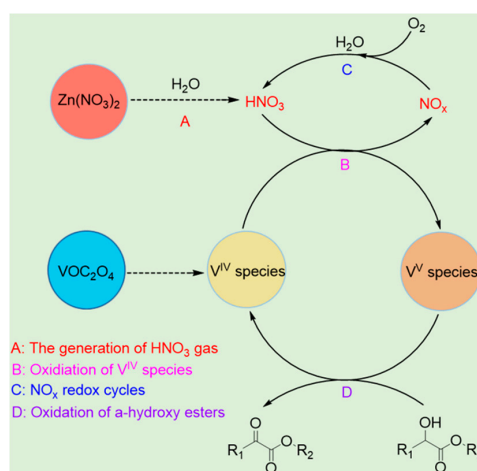

Figure 5. V 2p XPS spectra of the reaction mixture: V 2p XPS spectra of the $Zn(NO_3)_2$/VOC_2O_4 reaction mixture (a); and V 2p XPS spectra of the $Fe(NO_3)_3$/VOC_2O_4 reaction mixture (b).

Based on the above results and previous reports [19,20], the reaction mechanism for $Zn(NO_3)_2$/VOC_2O_4 catalyzed aerobic oxidation of α-hydroxy esters is proposed in Scheme 1. Firstly, the interaction of VOC_2O_4 and $Zn(NO_3)_2$ occurred under such oxidative conditions. In the presence of water, the oxidative gas of HNO_3 was generated after the interaction of VOC_2O_4 with $Zn(NO_3)_2$. Then, vanadium (IV) species derived from VOC_2O_4 underwent oxidation to vanadium (V) species by HNO_3 gas, and after that the active vanadium (V) species oxidized α-hydroxy esters to α-keto esters with the formation of vanadium (IV) species. In this oxidation reaction, the oxidative gas of HNO_3 generated in this catalyst system is expected to initiate and sustain vanadium (IV)/vanadium (V) redox cycle, and molecular oxygen plays an important role in NO_x redox cycle. Such proposed reaction mechanism could explain the above experimental phenomena.

Scheme 1. Plausible reaction mechanism for $Zn(NO_3)_2$/VOC_2O_4 catalyzed aerobic oxidation of α-hydroxy esters.

3. Materials and Methods

3.1. Catalyst Preparation

$VOC_2O_4·2H_2O$ was synthesized according to literature procedure [40]. Typically, vanadium pentoxide (2.0 g), oxalic acid dihydrate (4.3 g) and glacial acetic acid (16.8 mL) were added to a flask (50 mL). The reaction mixture was stirred for 2 h at 110 °C. The resulting slurry was cooled to room temperature, filtered, and the filtrate was discarded. The solid was dried at 80 °C under a vacuum for 5 h. The FT-IR spectrum of $VOC_2O_4·2H_2O$ is presented in Figure S1.

3.2. Typical Procedures of Reaction

In a typical procedure for catalytic oxidation α-hydroxy esters, α-hydroxy esters (5 mmol), $VOC_2O_4·2H_2O$ (0.25 mmol), $Zn(NO_3)_2·6H_2O$ (0.25 mmol), and CH_3CN (5 mL) were placed in autoclave (25 mL). Oxygen was then added (0.2 MPa). The mixture was stirred at 80 °C for 1.5 h. After the reaction was completed, the resulting mixture was filtered and determined by gas chromatography (GC-7900 equipped with FID detector and PEG-20 capillary column, Techcomp Ltd, Shanghai, China) Conversion and selectivity were determined based on area normalization method. Products were verified by GC-MS, NMR and ATR-IR.

3.3. Typical Procedures of Analysis Method

GC-MS was performed on a Thermo Fisher Trace 1300s-ISQ LT instrument (Thermo Fisher, Waltham, MA, USA) with electron ionization (EI) mass spectrometry. NMR spectra were recorded at 500 MHz with Bruker Avance III HD instrument (Bruker, Billerica, MA, USA) using $CDCl_3$ as the solvent with tetramethylsilane (TMS) as the internal standard.

The FT-IR spectra were recorded within a 4000–500 cm^{-1} region on a Thermo Fisher Nicolet iN10 MX & iS10 infrared spectrometer (Thermo Fisher, Waltham, MA, USA) using KBr pellets.

The UV–vis spectra was recorded within a 200–800 nm region on an Agilent Cary 60 spectrophotometer (Agilent, Palo Alto, CA, USA) with quartz cells at room temperature.

XPS measurements were performed on a Thermo Fisher ESCALAB 250Xi spectrometer (Thermo Fisher, Waltham, MA, USA).

The situ ATR-IR spectra were recorded within a 3000–600 cm^{-1} region on a Mettler Toledo React IR15 spectrometer (Mettler Toledo, Zurich, Switzerland) equipped with a liquid-nitrogen-cooled MCT (mercury cadmium telluride) detector and a diamond probe. The typical experiments were carried out in a closed flask. The IR probe was immersed in liquid phase reaction mixture or gas phase.

4. Conclusions

An efficient catalytic system consisting of $Zn(NO_3)_2/VOC_2O_4$ was developed for aerobic oxidation of α-hydroxy esters. Methyl DL-mandelate or methyl lactate could be facilely oxidized into its corresponding α-keto ester with high yields (up to 99% conversion of α-hydroxy esters) even under normal pressure at room temperature. $Zn(NO_3)_2$ combined with VOC_2O_4 exhibited unique catalytic activity compared to other tested metal nitrates such as $Fe(NO_3)_3$. Different nitric species were generated after interaction of VOC_2O_4 with $Zn(NO_3)_2$ or $Fe(NO_3)_3$. The coordination complex was identified by UV-vis and ATR-IR indicated the unique reaction route in $Zn(NO_3)_2/VOC_2O_4$, which gave diverse nitric oxidative gas with different oxidizing ability. The XPS result suggested that HNO_3 gas derived from the interaction of $Zn(NO_3)_2$ with VOC_2O_4 could promote the oxidation of VOC_2O_4 to generate active vanadium (V) species. Further development of efficient vanadium-based catalysts for oxidation of alcohols is currently underway.

Supplementary Materials: The supplementary materials are available online, Figure S1: FT-IR spectrum of vanadyl oxalate, Figure S2: UV–vis spectra of $Zn(NO_3)_2$ or $Fe(NO_3)_3$ in CH_3CN solvent, Figure S3: ATR-IR spectra in the C-N region of $Zn(NO_3)_2$ or $Fe(NO_3)_3$ in CH_3CN solvent, Figures S4 and S5: NMR spectra of products, Figures S6–S9: MS spectra of products, Figures S10–S17: Original spectra of GC. Table S1: The effect of catalyst

loading and $Zn(NO_3)_2$ loading for catalytic oxidation of methyl DL-mandelate, Table S2: Catalytic oxidation of various alcohols.

Author Contributions: Y.J., C.X. and X.L. investigated literature; Y.J. performed the experiments and analyzed the data; and Z.D. and S.L. wrote and approved the paper.

Conflicts of Interest: The authors declare no conflict of interest.

References

1. Guo, L.N.; Wang, H.; Duan, X.H. Recent advances in catalytic decarboxylative acylation reactions via a radical process. *Org. Biomol. Chem.* **2016**, *14*, 7380–7391. [CrossRef]
2. Haanan, T.S.; Wuppertal, H.T.; Gologne, G.B.; Odenthal, H.U.B. Preparation of 3,6-disubstituted 4-amino-1,2,4-triazin-5-ones. U.S. Patent 4408044, 4 October 1983.
3. Maki-Arvela, P.; Simakova, I.L.; Salmi, T.; Murzin, D.Y. Production of lactic acid/lactates from biomass and their catalytic transformations to commodities. *Chem. Rev.* **2014**, *114*, 1909–1971. [CrossRef]
4. Vadagaonkar, K.S.; Kalmode, H.P.; Shinde, S.L.; Chaskar, A.C. An efficient and metal-free synthesis of α-ketoesters via oxidative cross coupling of arylglyoxals with alcohols. *Chem. Sel.* **2017**, *2*, 900–903.
5. Xu, X.; Ding, W.; Lin, Y.; Song, Q. Cu-Catalyzed aerobic oxidative esterification of acetophenones with alcohols to α-ketoesters. *Org. Lett.* **2015**, *17*, 516–519. [CrossRef]
6. Zhang, C.; Feng, P.; Jiao, N. Cu-Catalyzed esterification reaction via aerobic oxygenation and C-C bond cleavage: An approach to α-Ketoesters. *J. Am. Chem. Soc.* **2013**, *135*, 15257–15262. [CrossRef]
7. Liu, K.; Huang, X.; Pidko, E.A.; Hensen, E.J.M. MoO_3-TiO_2 synergy in oxidative dehydrogenation of lactic acid to pyruvic acid. *Green Chem.* **2017**, *19*, 3014–3022. [CrossRef]
8. Zhang, W.; Ensing, B.; Rothenberg, G.; Shiju, N.R. Designing effective solid catalysts for biomass conversion: Aerobic oxidation of ethyl lactate to ethyl pyruvate. *Green Chem.* **2018**, *20*, 1866–1873. [CrossRef]
9. Csjernyik, G.; Ell, A.H.; Fadini, L.; Pugin, B.; Backvall, J.E. Efficient ruthenium-catalyzed aerobic oxidation of alcohols using a biomimetic coupled catalytic system. *J. Org. Chem.* **2002**, *67*, 1657–1662. [CrossRef]
10. Furukawa, K.; Inada, H.; Shibuya, M.; Yamamoto, Y. Chemoselective conversion from α-hydroxy acids to α-keto acids enabled by nitroxyl-radical-catalyzed aerobic oxidation. *Org. Lett.* **2016**, *18*, 4230–4233. [CrossRef]
11. Gorbanev, Y.Y.; Klitgaard, S.K.; Woodley, J.M.; Christensen, C.H.; Riisager, A. Gold-catalyzed aerobic oxidation of 5-hydroxymethylfurfural in water at ambient temperature. *ChemSusChem* **2009**, *2*, 672–675. [CrossRef]
12. Sugiyama, S.; Kikumoto, T.; Tanaka, H.; Nakagawa, K.; Sotowa, K.I.; Maehara, K.; Himeno, Y.; Ninomiya, W. Enhancement of catalytic activity on Pd/C and Te-Pd/C during the oxidative dehydrogenation of sodium lactate to pyruvate in an aqueous phase under pressurized oxygen. *Catal. Lett.* **2009**, *131*, 129–134. [CrossRef]
13. Wang, X.; Liu, R.; Jin, Y.; Liang, X. TEMPO/HCl/NaNO₂ catalyst: A transition-metal-free approach to efficient aerobic oxidation of alcohols to aldehydes and ketones under mild conditions. *Chem. Eur. J.* **2008**, *14*, 2679–2685. [CrossRef]
14. Hirao, T. Vanadium in modern organic synthesis. *Chem. Rev.* **1997**, *97*, 2707–2724. [CrossRef]
15. Sutradhar, M.; Martins, L.M.D.R.S.; Silva, M.F.C.G.; Pombeiro, A.J.L. Vanadium complexes: Recent progress in oxidation catalysis. *Coord. Chem. Rev.* **2015**, *301*, 200–239. [CrossRef]
16. Kirihara, M.; Ochiai, Y.; Takizawa, S.; Takahata, H.; Nemoto, H. Aerobic oxidation of α-hydroxycarbonyls catalysed by trichlorooxyvanadium: Efficient synthesis of α-dicarbonyl compounds. *Chem. Commun.* **1999**, 1387–1388. [CrossRef]

17. Hanson, S.K.; Baker, R.T.; Gordon, J.C.; Scott, B.L.; Sutton, A.D.; Thorn, D.L. Aerobic oxidation of pinacol by vanadium(V) dipicolinate complexes: Evidence for reduction to vanadium (III). *J. Am. Chem. Soc.* **2009**, *131*, 428–429. [CrossRef]

18. Hanson, S.K.; Wu, R.; Silks, L.A.P. Mild and selective vanadium catalyzed oxidation of benzylic, allylic, and propargylic alcohols using air. *Org. Lett.* **2011**, *13*, 1908–1911. [CrossRef]

19. Du, Z.; Liu, J.; Lu, T.; Ma, Y.; Xu, J. Studies on the roles of vanadyl sulfate and sodium nitrite in catalytic oxidation of benzyl alcohol with molecular oxygen. *Sci. China Chem.* **2015**, *58*, 114–122. [CrossRef]

20. Ma, J.; Du, Z.; Xu, J.; Chu, Q.; Pang, Y. Efficient aerobic oxidation of 5-hydroxymethylfurfural to 2,5-diformylfuran, and synthesis of a fluorescent material. *ChemSusChem* **2011**, *4*, 51–54. [CrossRef]

21. Kodama, S.; Ueta, Y.; Yoshida, J.; Nomoto, A.; Yano, S.; Ueshima, M.; Ogawa, A. Tetranuclear vanadium complex, $(VO)_4(hpic)_4$: A recyclable catalyst for oxidation of benzyl alcohols with molecular oxygen. *Dalton Trans.* **2009**, *0*, 9708–9711. [CrossRef]

22. Maeda, Y.; Kakiuchi, N.; Matsumura, S.; Nishimura, T.; Kawamura, T.; Uemura, S. Oxovanadium complex-catalyzed aerobic oxidation of propargylic alcohols. *J. Org. Chem.* **2002**, *67*, 6718–6724. [CrossRef]

23. Velusamy, S.; Punniyamurthy, T. Novel vanadium-catalyzed oxidation of alcohols to aldehydes and ketones under atmospheric oxygen. *Org. Lett.* **2004**, *6*, 217–219. [CrossRef]

24. Dressen, M.H.C.L.; Stumpel, J.E.; Kruijs, B.H.P.; Meuldijk, J.; Vekemans, J.A.J.M.; Hulshof, L.A. The mechanism of the oxidation of benzyl alcohol by iron (III)nitrate: Conventional versus microwave heating. *Green Chem.* **2009**, *11*, 60–64. [CrossRef]

25. Hu, Y.; Chen, L.; Li, B. Fe(NO$_3$)$_3$/2,3-dichloro-5,6-dicyano-1,4-benzoquinone (DDQ): An efficient catalyst system for selective oxidation of alcohols under aerobic conditions. *Catal. Commun.* **2018**, *103*, 42–46. [CrossRef]

26. Ramos-Fernandez, E.V.; Geels, N.J.; Shiju, N.R.; Rothenberg, G. Titania-catalysed oxidative dehydrogenation of ethyl lactate: Effective yet selective free-radical oxidation. *Green Chem.* **2014**, *16*, 3358–3363. [CrossRef]

27. Yasukawa, T.; Ninomiya, W.; Ooyachi, K.; Aoki, N.; Mae, K. Efficient oxidative dehydrogenation of lactate to pyruvate using a gas-liquid micro flow system. *Ind. Eng. Chem. Res.* **2011**, *50*, 3858–3863. [CrossRef]

28. Zakzeski, J.; Bruijnincx, P.C.A.; Weckhuysen, B.M. In situ spectroscopic investigation of the cobalt-catalyzed oxidation of lignin model compounds in ionic liquids. *Green Chem.* **2011**, *13*, 671–680. [CrossRef]

29. Maeda, N.; Sano, S.; Mallat, T.; Hungerbuehler, K.; Baiker, A. Heterogeneous asymmetric hydrogenation of activated ketones: Mechanistic insight into the role of alcohol products by in situ modulation-excitation IR spectroscopy. *J. Phys. Chem. C* **2012**, *116*, 4182–4188. [CrossRef]

30. Sathyanarayana, D.N.; Patel, C.C. Studies on oxovanadium (IV) oxalate hydrates. *J. Inorg. Nucl. Chem.* **1965**, *27*, 297–302. [CrossRef]

31. Hester, R.E.; Scaife, C.W.J. Vibrational spectra of molten salts. III. infrared and raman spectra of variably hydrated zinc nitrate. *J. Chem. Phys.* **1967**, *47*, 5253–5258. [CrossRef]

32. Yang, H.S.; Finlayson-Pitts, B.J. Infrared spectroscopic studies of binary solutions of nitric acid and water and ternary solutions of nitric acid, sulfuric acid, and water at room temperature: Evidence for molecular nitric acid at the surface. *J. Phys. Chem. A* **2001**, *105*, 1890–1896. [CrossRef]

33. Bibart, C.H.; Ewing, G.E. Vibrationnal spectrum, torsional potential, and bonding of gaseous N_2O_4. *J. Chem. Phys.* **1974**, *61*, 1284–1292. [CrossRef]

34. Schaffert, R. The infrared absorption spectra of NO_2 and N_2O_4. *J. Chem. Phys.* **1933**, *1*, 507–511. [CrossRef]

35. Gvozdic, V.; Tomisic, V.; Butorac, V.; Simeon, V. Association of nitrate ion with metal cations in aqueous solution: A UV-Vis spectrometric and factor-analytical study. *Croat. Chem. Acta* **2009**, *82*, 553–558.

36. Addison, C.C.; Amos, D.W.; Sutton, D. Infrared and raman spectra of solutions of zinc cadmium and mercury (II) nitrates in acetonitrile. *J. Chem. Soc.* **1968**, 2285–2290. [CrossRef]

37. Addison, C.C.; Sutton, D. Ultraviolet spectra of anhydrous metal nitrates. *J. Chem. Soc.* **1966**, 1524–1528. [CrossRef]

38. Zhang, W.; Innocenti, G.; Oulego, P.; Gitis, V.; Wu, H.; Ensing, B.; Cavani, F.; Rothenberg, G.; Shiju, N.R. Highly selective oxidation of ethyl lactate to ethyl pyruvate catalyzed by mesoporous vanadia-titania. *ACS Catal.* **2018**, *8*, 2365–2374. [CrossRef]

39. Greenwood, N.N.; Earnshaw, A. *Chemistry of the Element*, 2nd ed.; Elsevier: Oxford, UK, 1997; pp. 406–472.

40.　Smith, W.N., Jr. Vanadyl oxalate compounds and process for producing same. U.S. Patent 3689515, 5 September 1972.

Sample Availability: Samples of the compounds are not available from the authors.